Hindawi Publishing Corporation
Journal of Chemistry
Volume 2014, Article ID 173902, 15 pages
http://dx.doi.org/10.1155/2014/173902

Research Article

Synthesis and Conformational Analysis of Sterically Congested (4*R*)-(−)-1-(2,4,6-Trimethylbenzenesulfonyl)-3-*n*-butyryl-4-*tert*-butyl-2-imidazolidinone: X-Ray Crystallography and Semiempirical Calculations

Ibrahim A. Al-Swaidan,[1] Adel S. El-Azab,[1,2] Amer M. Alanazi,[1] and Alaa A.-M. Abdel-Aziz[1,3]

[1] *Department of Pharmaceutical Chemistry, College of Pharmacy, King Saud University, Riyadh 11451, Saudi Arabia*
[2] *Department of Organic Chemistry, Faculty of Pharmacy, Al-Azhar University, Cairo 11884, Egypt*
[3] *Department of Medicinal Chemistry, Faculty of Pharmacy, University of Mansoura, Mansoura 35516, Egypt*

Correspondence should be addressed to Alaa A.-M. Abdel-Aziz; alaa_moenes@yahoo.com

Received 2 October 2013; Revised 4 November 2013; Accepted 7 November 2013; Published 5 January 2014

Academic Editor: Fernanda Carvalho

The crystal structure of (4*R*)-(−)-1-(2,4,6-trimethylbenzenesulfonyl)-3-*n*-butyryl-4-*tert*-butyl-2-imidazolidinone **(3)** was determined by single-crystal X-ray diffraction. Compound **3** crystallizes in triclinic system in space group $P1$ ($\neq 1$). The crystal data are $a = 10.6216(5)$ Å, $b = 16.532(1)$ Å, $c = 8.9572(9)$ Å, $\alpha = 91.193(6)^\circ$, $\beta = 93.849(6)^\circ$, $\gamma = 88.097(4)^\circ$, $V = 1568.2(2)$ Å^3, $Z = 3$, $D_{calc} = 1.253$ g/cm^3, $\mu(\text{CuK}\alpha) = 15.98$ cm^{-1}, $F_{000} = 636.00$, $T = 20.0^\circ$C, and $R = 0.037$. The crystal structure confirmed the occurrence of three molecules of **3A**, **3B**, and **3C** in which the *n*-butyryl moiety adopted the *s-transoid* conformation. Crystal structure also revealed that the conformation of 2,4,6-trimethylbenzenesulfonyl groups was in *anti*-position relative to *tert*-butyl group. The crystal packing showed that three molecules of compound **3** are stacked as a result of intermolecular π-π interactions between the phenyl ring of one molecule and the phenyl ring of the other molecule by approaching each other to an interplanar separation of 5.034 Å. Interestingly, these stacked molecules are also connected by intermolecular *CH*-π interaction. The conformational analysis of the *s-transoid* **3A**, **3B**, and **3C** was separately performed by molecular mechanic MM+ force field. Additionally, computational investigation using semiempirical AM1 and PM3 methods was performed to find a correlation between experimental and calculated geometrical parameters. The data obtained suggest that the structural data furnished by the AM1 method is in better agreement with those experimentally determined for the above compound. It has been found that the lowest energetic conformer computed gives approximate correspondence with experimental solid state data.

1. Introduction

The energy based conformational searching technique is a considerable computational request and is still an active area of research. When the property of interest is energy, the following methodology is indicated: full conformational search using molecular mechanics, followed by geometry optimization using semiempirical model for selected conformers, and finally single-point calculation using *ab* initio models for selected conformers [1]. On the other hand, steric bulkiness of chiral 2-imidazolidinones [2] plays an effective role in greatly enhancing stereoselectivity, and so sterically congested chiral 2-imidazolidinones [3–5] represent promising auxiliaries for providing excellent diastereocontrol. We reported the synthesis and chiral application of 4-*tert*-butyl-2-imidazolidinone which were greatly enhanced by the occurrence of *N*-arylsulfonyl fragments [4]. Moreover, several 2-imidazolidinone derivatives containing diarylsulfonylurea pharmacophore have been synthesized and screened for antitumor activity against various human solid tumors [6–17]. More interestingly the structure of the arylsulfonyl-2-imidazolidinone such as 4-benzamido-3-methyl-1-tosyl-2-imidazolidinone and (*S*)-(+)-1-[1-(4-aminobenzoyl) indoline-5-sulfonyl]-4-phenyl-4,5-dihydroimidazol-2-one has elucidat-

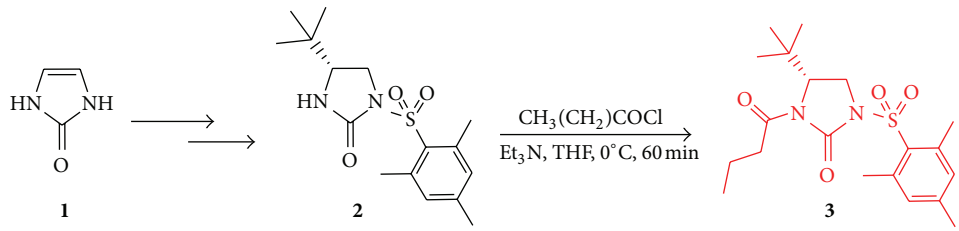

Scheme 1: Synthesis of (4*R*)-(−)-1-(2,4,6-Trimethylbenzenesulfonyl)-3-*n*-butyryl-4-*tert*-butyl-2-imidazolidinone (**3**).

ed using X-ray analysis [18, 19]. Recently, we reported about the X-ray analysis and computational studies of *trans*-1-acetyl-4,5-di-*tert*-butyl-2-imidazolidinone in which the crystal unit cell showed two independent molecules connected together by two intermolecular hydrogen bonds [20].

In such a way and in continuation of our previous report [20] we studied single-crystal X-ray and the theoretical conformational analysis of (4*R*)-(−)-1-(2,4,6-trimethylbenzenesulfonyl)-3-butyryl-4-*tert*-butyl-2-imidazolidinone (**3**), as a cyclic arylsulfonylurea, focusing on the configuration of substituents around the 2-imidazolidinone core and to establish the factors that influence this configuration and if this configuration can be predicted for new substituted 2-imidazolidinone.

2. Experimental

2.1. Procedure for Synthesis of (4R)-(−)-1-(2,4,6-Trimethylbenzenesulfonyl)-3-n-butyryl-4-tert-butyl-2-imidazolidinone ***(3)****.* n-Butyl lithium (1.5 M in hexane, 0.5 mmoL) was added to a stirred solution of compound **2** (0.5 mmoL) in THF (10 mL) at −78°C under nitrogen atmosphere for 10 min and n-butyryl chloride (1.0 mmoL) was added dropwise at −78°C. The reaction mixture was stirred at room temperature for 1 h and then was quenched by passing through silica gel (EtOAc, 100 mL), evaporated under vacuum, followed by column chromatography on silica gel (EtOAc: hexane) to afford compound **3** in quantitative yield.

Compound (4*R*)-**3** (97%): white crystals, mp 125–127°C (Hexane), IR (KBr) ν_{max}/cm^{-1}, 1736, 1701 (CO), 1320, 1175 (SO_2); $[\alpha]_D^{26} = -12.0^\circ$ (*c* 1.00, $CHCl_3$); ^{1}H-NMR ($CDCl_3$, 500 MHz): δ 6.99 (s, 2H), 4.42–4.40 (d, 1H, J = 8.5 Hz), 3.97–3.96 (d, 1H, J = 8.5 Hz), 3.85–3.81 (t, 1H, J = 8.5 Hz), 2.85–2.81 (m, 1H), 2.74–2.67 (m, 1H), 2.65 (s, 6H), 2.31 (s, 3H), 1.66–1.58 (m, 2H), 0.93 (s, 9H), and 0.92–0.88 (t, 3H, J = 7.3 Hz).

2.2. X-Ray Data Collection, Structure Solution, and Refinement for (4R)-(−)-1-(2,4,6-Trimethylbenzenesulfonyl)-3-n-butyryl-4-tert-butyl-2-imidazolidinone ***(3)***

2.2.1. Data Collection. (4*R*)-(-)-1-(2,4,6-Trimethylbenzenesulfonyl)-3-butyryl-4-*tert*-butyl-2-imidazolidinone (**3**) (Scheme 1) was prepared according to our previous report [4, 21]. A colorless plate crystal of $C_{20}H_{30}N_2O_4S$ having approximate dimensions of 0.25 × 0.10 × 0.25 mm was mounted on a glass fiber. All measurements were made on a Rigaku AFC7R diffractometer with graphite monochromated Cu-Kα radiation and a rotating anode generator. Cell constants and orientation matrix for data collection obtained from a least-squares refinement using the setting angles of 25° carefully centered reflections in the range $59.17^\circ < 2\theta < 59.87^\circ$ corresponded to a triclinic cell (Table 1).

The data were collected at a temperature of 20 ± 1°C using the $\omega - 2\theta$ scan technique to a maximum 2θ value of 120.1°. Omega scans of several intense reflections, made prior to data collection, had an average width at half-height of 0.28° with a take-off angle of 6.0°. Scans of $(1.78 + 0.30 \tan\theta)^\circ$ were made at a speed of 16.0°/min (in omega). The weak reflections ($I < 10.0\sigma(I)$) were rescanned (maximum of 5 scans) and the counts were accumulated to ensure good counting statistics. Stationary background counts were recorded on each side of the reflection. The ratio of peak counting time to background counting time was 2 : 1. The diameter of the incident beam collimator was 0.5 mm and the crystal to detector distance was 235 mm. The computer-controlled slits were set to 3.0 mm (horizontal) and 3.0 mm (vertical).

2.2.2. Data Reduction. Of the 4942 reflections which were collected, 4649 were unique ($R_{int} = 0.059$); equivalent reflections were merged. The intensities of three representative reflections were measured after every 150 reflections. The linear absorption coefficient, μ, for Cu-Kα radiation is 16.0 cm^{-1} and an empirical absorption correction based on azimuthal scans of several reflections was applied which resulted in transmission factors ranging from 0.81 to 1.00. The data were corrected for Lorentz and polarization effects and a correction for secondary extinction were applied (coefficient = $6.35905e^{-06}$).

2.2.3. Structure Solution and Refinement. The structure was solved by direct methods [22] and expanded using Fourier techniques [23]. The nonhydrogen atoms were refined anisotropically and hydrogen atoms were included but not refined. The final cycle of full-matrix least-squares refinement (Least-squares: function minimized: $\sum \omega(|Fo| - |Fc|)^2$, where $w = 1/\sigma^2(Fo) = [\sigma_c^2(Fo) + (p^2/4)Fo^2]^{-1}$ and $\sigma_c^2(Fo)$ = e.s.d. based on counting, p = p-factor) was based on 4409 observed reflections ($I > 3.00\sigma(I)$) and 729 variable parameters and converged (largest parameter shift was 0.09

Table 1: Summary of crystal data, intensity data collection, and structure refinement for compound **3** at 20.0°C.

(a) Crystal data

Empirical formula	$C_{20}H_{30}N_2O_4S$
Formula weight	394.53
Crystal color, Habit	Colorless, plate
Crystal dimensions	0.25 × 0.10 × 0.25 mm
Crystal system	Triclinic
Lattice type	Primitive
No. of reflections used for unit cell Determination (2θ range)	25 (59.2–59.9°)
Omega scan peak width at half-height	0.28°
Lattice parameters	a = 10.6216(5) Å b = 16.532(1) Å c = 8.9572(9) Å α = 91.193(6)° β = 93.849(6)° γ = 88.097(4)° V = 1568.2(2) Å^3
Space group	P1 (#1)
Z value	3
D_{calc}	1.253 g/cm^3
F_{000}	636.00
μ (CuKα)	15.98 cm^{-1}

(b) Intensity measurements

Diffractometer	Rigaku AFC7R
Radiation	CuKα (λ = 1.54178 Å) Graphite monochromated
Attenuator	Ni foil (factor = 8.82)
Take-off angle	6.0°
Detector aperture	3.0 mm horizontal 3.0 mm vertical
Crystal to detector distance	235 mm
Voltage, current	35 kV, 150 mA
Temperature	20.0°C
Scan type	$\omega - 2\theta$
Scan rate	16.0°/min (in ω) (up to 5 scans)
Scan Width	$(1.78 + 0.30 \tan\theta)$°
$2\theta_{max}$	120.1°
No. of reflections measured	Total: 4942 Unique: 4649 (R_{int} = 0.059)

(c) Structure solution and refinement

Structure solution	Direct methods (SIR92)
Refinement	Full-matrix least-squares
P factor	0.0800
Anomalous dispersion	All nonhydrogen atoms
No. of observations ($I > 3.00\sigma(I)$)	4409
No. of variables	729
Reflection/parameter ratio	6.05
Residuals: R; Rw	0.037; 0.056
Residuals $R1$	0.037
No. of reflections to calc $R1$	4409
Goodness of fit indicator	1.26
Max shift/error in final cycle	0.09
Maximum peak in final diff. map	0.15 e$^-$/Å^3
Minimum peak in final diff. map	−0.20 e$^-$/Å^3

times its esd) with unweighted and weighted agreement factors of

$$R = \frac{\sum ||\text{Fo}| - |\text{Fc}||}{\sum |\text{Fo}|} = 0.037,$$
$$R\omega = \sqrt{\frac{\sum \omega(|\text{Fo}| - |\text{Fc}|)^2}{\sum \omega \text{Fo}^2}} = 0.056. \quad (1)$$

The standard deviation of an observation of unit weight (standard deviation of an observation of unit weight: $\sqrt{\sum \omega(|\text{Fo}| - |\text{Fc}|)^2/(\text{No} - \text{Nv})}$, where: no. = number of observations and nv = number of variables) was 1.26 and the weighting scheme was based on counting statistics and included a factor (P = 0.080) to down-weight the intense reflections. Plots of $\sum \omega(|\text{Fo}| - |\text{Fc}|)^2$ versus |Fo|, reflection order in data collection, $\sin\theta/\lambda$, and various classes of indices showed no unusual trends. The maximum and minimum peaks on the final difference Fourier map corresponded to 0.15 and −0.20 $e^-/\text{Å}^3$, respectively.

Neutral atom scattering factors were taken from Cromer and Waber [24] and anomalous dispersion effects were included in Fcalc [25]; the values for $\Delta f'$ and $\Delta f''$ were those of Creagh and McAuley [26]. The values for the mass attenuation coefficients are those of Creagh and McAuley [26]. All calculations were performed using the teXsan [27] crystallographic software package of Molecular Structure Corporation and crystal data summary is given in Table 1. The selected bond lengths, angles, and torsion angles are given in Tables 2–4 and the molecular structure with the atom-numbering scheme and the packing within the cell lattice are shown in Figures 1 and 3, respectively.

2.3. Computational Calculations. All molecular modeling calculations were performed using HyperChem version 8.0.6 [28], running on "Windows Vista" operating system installed on an Intel core 2 duo PC with a 2.66 GHz processor and 2000 Mb RAM.

2.3.1. Conformational Search. Conformational analyses of isolated molecule **3** (**3A**, **3B**, and **3C**) were done in the same way using the procedure which is suggested for conformational flexible compounds when the property of interest is energy [1]. Initial X-ray structures for the molecules **3A**, **3B** and **3C** were used for conformational analysis with HyperChem 8.0 [28]. The MM+ [29] (calculations in vacuum,

Table 2: Experimental bond lengths (Å).

Atom	Atom	Distance	Atom	Atom	Distance
S1A	O3A	1.416(3)	S1A	O4A	1.428(3)
S1A	N2A	1.671(3)	S1A	C12A	1.777(4)
S1B	O3B	1.430(4)	S1B	O4B	1.421(4)
S1B	N2B	1.664(3)	S1B	C12B	1.773(4)
S1C	O3C	1.416(3)	S1C	O4C	1.425(3)
S1C	N2C	1.669(3)	S1C	C12C	1.768(4)
O1A	C4A	1.215(5)	O1B	C4B	1.219(5)
O1C	C4C	1.210(5)	O2A	C1A	1.200(4)
O2B	C1B	1.209(5)	O2C	C1C	1.203(5)
N1A	C1A	1.376(5)	N1A	C2A	1.485(5)
N1A	C4A	1.408(5)	N1B	C1B	1.380(5)
N1B	C2B	1.485(5)	N1B	C4B	1.401(5)
N1C	C1C	1.386(5)	N1C	C2C	1.476(5)
N1C	C4C	1.413(5)	N2A	C1A	1.395(5)
N2A	C3A	1.469(5)	N2B	C1B	1.386(5)
N2B	C3B	1.473(5)	N2C	C1C	1.386(5)
N2C	C3C	1.486(5)	C2A	C3A	1.523(5)
C2A	C8A	1.556(6)	C2B	C3B	1.531(5)
C2B	C8B	1.549(5)	C2C	C3C	1.520(5)
C2C	C8C	1.550(5)	C4A	C5A	1.507(6)
C4B	C5B	1.503(6)	C4C	C5C	1.486(6)
C5A	C6A	1.531(6)	C5B	C6B	1.507(7)
C5C	C6C	1.516(6)	C6A	C7A	1.490(8)
C6B	C7B	1.476(9)	C6C	C7C	1.492(9)
C8A	C9A	1.533(7)	C8A	C10A	1.533(6)
C8A	C11A	1.502(7)	C8B	C9B	1.515(7)
C8B	C10B	1.530(6)	C8B	C11B	1.508(7)
C8C	C9C	1.515(8)	C8C	C10C	1.523(6)
C8C	C11C	1.532(7)	C12A	C13A	1.401(5)
C12A	C17A	1.411(6)	C12B	C13B	1.412(6)
C12B	C17B	1.407(6)	C12C	C13C	1.410(6)
C12C	C17C	1.403(6)	C13A	C14A	1.383(6)
C13A	C18A	1.502(6)	C13B	C14B	1.408(7)
C13B	C18B	1.487(7)	C13C	C14C	1.404(6)
C13C	C18C	1.502(6)	C14A	C15A	1.377(6)
C14B	C15B	1.372(7)	C14C	C15C	1.355(7)
C15A	C16A	1.363(6)	C15A	C19A	1.500(6)
C15B	C16B	1.376(7)	C15B	C19B	1.507(8)
C15C	C16C	1.368(7)	C15C	C19C	1.503(7)
C16A	C17A	1.396(6)	C16B	C17B	1.392(7)
C16C	C17C	1.404(6)	C17A	C20A	1.500(6)
C17B	C20B	1.506(7)	C17C	C20C	1.506(6)

bond dipole option for electrostatics, and RMS gradient of 0.01 kcal/mol) conformational searching in torsional space was performed using the multiconformer method [30, 31]. Each molecule **3A**, **3B**, and **3C** was subjected to a separate conformational search and the most stable conformer was energy minimized using semiempirical MO methods AM1 [32] and PM3 [33] included in MOPAC version 2009 [34] using HyperChem as GUI. Vibration frequencies calculation for each conformer was characterized to be the stable structure (no imaginary frequencies).

3. Results and Discussion

As a result of the potential conformational flexibility of the substituent groups of compound **3**, we have used solid

Table 3: Experimental bond angles (deg).

Atom	Atom	Atom	Angle	Atom	Atom	Atom	Angle
O3A	S1A	O4A	118.5(2)	O3A	S1A	N2A	108.4(2)
O3A	S1A	C12A	110.8(2)	O4A	S1A	N2A	102.9(2)
O4A	S1A	C12A	110.6(2)	N2A	S1A	C12A	104.3(2)
O3B	S1B	O4B	117.6(2)	O3B	S1B	N2B	103.7(2)
O3B	S1B	C12B	110.8(2)	O4B	S1B	N2B	108.8(2)
O4B	S1B	C12B	110.5(2)	N2B	S1B	C12B	104.3(2)
O3C	S1C	O4C	118.2(2)	O3C	S1C	N2C	107.7(2)
O3C	S1C	C12C	110.1(2)	O4C	S1C	N2C	103.9(2)
O4C	S1C	C12C	111.2(2)	N2C	S1C	C12C	104.7(2)
C1A	N1A	C2A	111.9(3)	C1A	N1A	C4A	126.2(3)
C2A	N1A	C4A	120.4(3)	C1B	N1B	C2B	111.0(3)
C1A	N1B	C4B	126.4(3)	C2B	N1B	C4B	120.5(3)
C1C	N1C	C2C	111.7(3)	C1C	N1C	C4C	126.4(3)
C2C	N1C	C4C	120.5(3)	S1A	N2A	C1A	122.1(2)
S1A	N2A	C3A	124.5(2)	C1A	N2A	C3A	111.1(3)
S1B	N2B	C1B	122.6(3)	S1B	N2B	C3B	124.5(3)
C1B	N2B	C3B	111.3(3)	S1C	N2C	C1C	121.7(3)
S1C	N2C	C3C	125.4(3)	C1C	N2C	C3C	111.0(3)
O2A	C1A	N1A	128.9(3)	O2A	C1A	N2A	124.4(3)
N1A	C1A	N2A	106.7(3)	O2B	C1B	N1B	127.9(4)
O2B	C1B	N2B	124.7(4)	N1B	C1B	N2B	107.4(3)
O2C	C1C	N1C	128.0(4)	O2C	C1C	N2C	125.4(4)
N1C	C1C	N2C	106.6(3)	N1A	C2A	C3A	101.0(3)
N1A	C2A	C8A	113.5(3)	C3A	C2A	C8A	113.2(3)
N1B	C2B	C3B	101.6(3)	N1B	C2B	C8B	113.8(3)
C3B	C2B	C8B	114.6(3)	N1C	C2C	C3C	101.7(3)
N1C	C2C	C8C	114.6(3)	C3C	C2C	C8C	113.4(3)
N2A	C3A	C2A	103.3(3)	N2B	C3B	C2B	102.7(3)
N2C	C3C	C2C	102.2(3)	O1A	C4A	N1A	119.0(4)
O1A	C4A	C5A	122.7(4)	N1A	C4A	C5A	118.2(3)
O1B	C4B	N1B	119.1(4)	O1B	C4B	C5B	122.4(4)
N1B	C4B	C5B	118.4(3)	O1C	C4C	N1C	118.1(4)
O1C	C4C	C5C	123.5(4)	N1C	C4C	C5C	118.4(3)
C4A	C5A	C6A	111.4(4)	C4B	C5B	C6B	112.3(4)
C4C	C5C	C6C	112.5(4)	C5A	C6A	C7A	111.6(4)
C5B	C6B	C7B	112.3(5)	C5C	C6C	C7C	112.9(4)
C2A	C8A	C9A	110.3(4)	C2A	C8A	C10A	106.3(4)
C2A	C8A	C11A	113.9(3)	C9A	C8A	C10A	108.2(4)
C9A	C8A	C11A	108.0(5)	C10A	C8A	C11A	110.1(4)
C2B	C8B	C9B	110.9(3)	C2B	C8B	C10B	106.3(4)
C2B	C8B	C11B	112.0(3)	C9B	C8B	C10B	109.9(4)
C9B	C8B	C11B	107.9(4)	C10B	C8B	C11B	109.8(4)
C2C	C8C	C9C	110.8(4)	C2C	C8C	C10C	107.4(3)
C2C	C8C	C11C	111.8(3)	C9C	C8C	C10C	108.5(4)
C9C	C8C	C11C	108.6(5)	C10C	C8C	C11C	109.7(4)
S1A	C12A	C13A	118.1(3)	S1A	C12A	C17A	120.4(3)
C13A	C12A	C17A	121.4(4)	S1B	C12B	C13B	120.3(3)
S1B	C12B	C17B	118.3(3)	C13B	C128	C17B	121.3(4)
S1C	C12C	C13C	118.4(3)	S1C	C12C	C17C	120.7(3)
C13C	C12C	C17C	120.8(4)	C12A	C13A	C14A	117.5(4)

Table 3: Continued.

Atom	Atom	Atom	Angle	Atom	Atom	Atom	Angle
C12A	C13A	C18A	125.7(4)	C14A	C13A	C18A	116.8(4)
C12B	C13B	C14B	117.2(4)	C12B	C13B	C18B	127.2(4)
C14B	C13B	C18B	115.6(4)	C12C	C13C	C14C	117.8(4)
C12C	C13C	C18C	125.2(4)	C14C	C13C	C18C	117.0(4)
C13A	C14A	C15A	122.9(4)	C13B	C14B	C15B	122.4(4)
C13C	C14C	C15C	122.3(4)	C14A	C15A	C16A	118.2(4)
C14A	C15A	C19A	121.1(4)	C16A	C15A	C19A	120.6(4)
C14B	C15B	C16B	118.6(4)	C14B	C15B	C19B	120.2(5)
C16B	C15B	C19B	121.2(5)	C14C	C15C	C16C	118.9(4)
C14C	C15C	C19C	121.5(5)	C16C	C15C	C19C	119.6(4)
C15A	C16A	C17A	123.1(4)	C15B	C16B	C17B	122.8(4)
C15C	C16C	C17C	122.8(4)	C12A	C17A	C16A	116.8(4)
C12A	C17A	C20A	126.3(4)	C16A	C17A	C20A	116.9(4)
C12B	C17B	C16B	117.6(4)	C12B	C17B	C20B	125.4(4)
C16B	C17B	C20B	117.0(4)	C12C	C17C	C16C	117.2(4)
C12C	C17C	C20C	126.7(4)	C16C	C17C	C20C	116.1(4)

state molecular structures (as obtained from single crystal X-ray diffraction analysis) to obtain realistic structure as starting geometries for the quantum chemical calculations. Additionally, the data obtained by X-ray diffraction analysis shed light on some interesting features of its molecular structures. Some structural characteristics of compound **3** are the geometrical parameters around the ring nitrogen atoms such as the relative orientation of the *n*-butyryl and the 2,4,6-trimethylbenzenesulfonyl groups at N1 and N2 positions. Although, the preferred conformation in the solid phase can be different from the solution structure and in gas phase, the X-ray diffraction data are useful for comparative purposes. Overall, the combination of experimental and computational results can help in understanding the physical and chemical properties of this molecule.

3.1. X-Ray Crystal Structure of (4R)-(−)-1-(2,4,6-Trimethylbenzenesulfonyl)-3-n-butyryl-4-tert-butyl-2-imidazolidinone (3). The molecular solid state structure of **3** and numbering system are indicated in Figure 1. Geometrical parameters for compound **3** are collected in Tables 2–4. In the crystal structure, compound **3** crystallizes in the *P*1 space group (Table 1) and exists in three independent conformationally different molecules in the unit cell (**3A**, **3B**, and **3C**; see Figures 1, 2, and 3). Recently, crystal structures having more than one molecule in the unit cell have aroused interest, since these compounds can help in understanding the interactions responsible for packing as well as to guide the design of technologically useful materials [35]. The three molecules present, certain disorder in the core 2-imidazolidinone and the substituents linked to such ring. Thus, there is some ambiguity in the atomic positions of the 2-imidazolidinone skeleton, *tert*-butyl, *n*-butyryl, and 2,4,6-trimethylbenzenesulfonyl groups of three molecules: **3A**, **3B**, and **3C**. These disorders are expected due to the conformational flexibility of the *tert*-butyl, *n*-butyryl, and 2,4,6-trimethylbenzenesulfonyl moieties. The five-membered imidazolidinone ring assumes distorted envelope conformation (half-chair;LISLOO) which may be related to angle strain (angle strain is calculated as the difference between the internal angle and the ideal sp^3 angle of 109.5°) [36]. Atoms system ∠N2–C3–C2 of **3A**, **3B**, and **3C** are deviated from ideal sp^3 angle by 6.2°, 6.8°, and 7.3°, respectively. Similarly ∠C3–C2–N1 system of **3A**, **3B**, and **3C** deviates by 8.5°, 7.9°, and 7.8°, respectively, from the ideal value [17, 18, 20, 36–41]. The same pattern was observed with angle system ∠N2–C2–N2. The structures of **3A**, **3B**, and **3C** depicted in Figures 1–3 are those more likely on the basis of standard bond distances and angles [17, 18, 20, 41]. In the three molecules (**3A**, **3B** and **3C**), the geometrical parameters of the 2-imidazolidinone ring are quite similar with few distortions (Tables 2–4). The geometries of ∠C4–N1–C2 and ∠C4–N1–C1 atoms are almost planar rather than the most stable pyramidal form with bond angles of ca. 120°–126° for the three molecules **3A**, **3B**, and **3C**. Similarly the geometries of ∠S1–N2–C1 and ∠S1–N2–C3 are also planar with bond angles ca. as 122.1° (**3A**), 122.6° (**3B**), 121.7° (**3C**), 124.5° (**3A** and **3B**), and 125.4° (**3C**), respectively [17, 18, 20, 38–41]. This geometry makes the two nitrogen atoms in each molecule distinguishable from a geometrical point of view. Moreover, the planarity angle ∠N2–C1–N1–C4 of molecules **3A**, **3B**, and **3C** was deviated from the planar urea form by 23°–26° with ca −154.1°, −150.9°, and −157.1°, respectively [20, 41–44]. It must be indicated that the two nitrogen atoms in each molecules occupy *anti*-positions relative to the mean plane of the ring system. This *anti*-position of both nitrogen atoms in each molecule is one of the reasons which make the central ring nonplanar [20]. This distortion leads to *trans*-geometry of *n*-butyryl fragment around one nitrogen atom and the sulfonyl moiety of the other nitrogen atom. As expected from the previous results [20], as a result of electron distribution, flexibility, and

Table 4: Experimental dihedral angles (deg).

Atom	Atom	Atom	Atom	Angle	Atom	Atom	Atom	Atom	Angle
S1A	N2A	C1A	O2A	20.7(5)	S1A	N2A	C1A	N1A	−158.4(2)
S1A	N2A	C3A	C2A	144.3(3)	S1A	C12A	C13A	C14A	174.9(3)
S1A	C12A	C13A	C18A	−4.1(5)	S1A	C12A	C17A	C16A	−175.1(3)
S1A	C12A	C17A	C20A	5.4(6)	S1B	N2B	C1B	O2B	17.4(5)
S1B	N2B	C1B	N1B	−162.1(3)	S1B	N2B	C3B	C2B	148.0(3)
S1B	C12B	C13B	C14B	−178.1(3)	S1B	C12B	C13B	C18B	2.7(6)
S1B	C12B	C17B	C16B	177.0(3)	S1B	C12B	C17B	C20B	−3.4(5)
S1C	N2C	C1C	O2C	23.1(6)	S1C	N2C	C1C	N1C	−156.5(3)
S1C	N2C	C3C	C2C	142.4(3)	S1C	C12C	C13C	C14C	175.0(3)
S1C	C12C	C13C	C18C	−5.3(6)	S1C	C12C	C17C	C16C	−173.8(3)
S1C	C12C	C17C	C20C	5.8(6)	O1A	C4A	N1A	C1A	167.1(4)
O1A	C4A	N1A	C2A	2.6(6)	O1A	C4A	C5A	C6A	0.1(6)
O1B	C4B	N1B	C1B	170.5(4)	O1B	C4B	N1B	C2B	8.5(5)
O1B	C4B	C5B	C6B	−13.6(6)	O1C	C4C	N1C	C1C	170.2(4)
O1C	C4C	N1C	C2C	4.7(6)	O1C	C4C	C5C	C6C	4.0(7)
O2A	C1A	N1A	C2A	−167.5(4)	O2A	C1A	N1A	C4A	26.8(6)
O2A	C1A	N2A	C3A	−175.7(4)	O2B	C1B	N1B	C2B	−167.0(4)
O2B	C1B	N1B	C4B	29.6(6)	O2B	C1B	N2B	C3B	−176.3(4)
O2C	C1C	N1C	C2C	−170.1(4)	O2C	C1C	N1C	C4C	23.3(6)
O2C	C1C	N2C	C3C	−171.9(4)	O3A	S1A	N2A	C1A	48.6(3)
O3A	S1A	N2A	C3A	−112.6(3)	O3A	S1A	C12A	C13A	171.4(3)
O3A	S1A	C12A	C17A	−10.7(4)	O3B	S1B	N2B	C1B	178.1(3)
O3B	S1B	N2B	C3B	13.6(4)	O3B	S1B	C12B	C13B	−142.5(3)
O3B	S1B	C12B	C17B	38.3(3)	O3C	S1C	N2C	C1C	42.0(3)
O3C	S1C	N2C	C3C	−120.7(3)	O3C	S1C	C12C	C13C	170.4(3)
O3C	S1C	C12C	C17C	−12.7(4)	O4A	S1A	N2A	C1A	174.9(3)
O4A	S1A	N2A	C3A	13.6(4)	O4A	S1A	C12A	C13A	38.0(3)
O4A	S1A	C12A	C17A	−144.1(3)	O4B	S1B	N2B	C1B	52.1(4)
O4B	S1B	N2B	C3B	−112.4(3)	O4B	S1B	C12B	C13B	−10.3(4)
O4B	S1B	C12B	C17B	170.5(3)	O4C	S1C	N2C	C1C	168.2(3)
O4C	S1C	N2C	C3C	5.4(4)	O4C	S1C	C12C	C13C	37.5(4)
O4C	S1C	C12C	C17C	−145.6(3)	N1A	C1A	N2A	C3A	5.2(4)
N1A	C2A	C3A	N2A	23.3(4)	N1A	C2A	C8A	C9A	54.5(5)
N1A	C2A	C8A	C10A	171.6(4)	N1A	C2A	C8A	C11A	−67.1(5)
N1A	C4A	C5A	C6A	176.7(4)	N1B	C1B	N2B	C3B	4.2(4)
N1B	C2B	C3B	N2B	23.2(4)	N1B	C2B	C8B	C9B	56.9(5)
N1B	C2B	C8B	C10B	176.3(4)	N1B	C2B	C8B	C11B	−63.7(5)
N1B	C4B	C5B	C6B	162.9(4)	N1C	C1C	N2C	C3C	8.5(4)
N1C	C2C	C3C	N2C	25.1(4)	N1C	C2C	C8C	C9C	52.0(5)
N1C	C2C	C8C	C10C	170.3(4)	N1C	C2C	C8C	C11C	−69.3(5)
N1C	C4C	C5C	C6C	−178.1(4)	N2A	S1A	C12A	C13A	−72.1(3)
N2A	S1A	C12A	C17A	105.8(3)	N2A	C1A	N1A	C2A	11.6(4)
N2A	C1A	N1A	C4A	−154.1(4)	N2A	C3A	C2A	C8A	−98.4(4)
N2B	S1B	C12B	C13B	106.4(3)	N2B	S1B	C12B	C17B	−72.7(3)
N2B	C1B	N1B	C2B	12.4(4)	N2B	C1B	N1B	C4B	−150.9(3)
N2B	C3B	C2B	C8B	−99.9(4)	N2C	S1C	C12C	C13C	−74.1(3)
N2C	S1C	C12C	C17C	102.9(3)	N2C	C1C	N1C	C2C	9.5(4)
N2C	C1C	N1C	C4C	−157.1(3)	N2C	C3C	C2C	C8C	−98.5(3)
C1A	N1A	C2A	C3A	−22.4(4)	C1A	N1A	C2A	C8A	99.1(4)
C1A	N1A	C4A	C5A	−9.6(6)	C1A	N2A	S1A	C12A	−69.5(3)
C1A	N2A	C3A	C2A	−18.8(4)	C1B	N1B	C2B	C3B	−22.8(4)

Table 4: Continued.

Atom	Atom	Atom	Atom	Angle	Atom	Atom	Atom	Atom	Angle
C1B	N1B	C2B	C8B	100.9(4)	C1B	N1B	C4B	C5B	−6.1(6)
C1B	N2B	S1B	C12B	−65.9(3)	C1B	N2B	C3B	C2B	−18.0(4)
C1C	N1C	C2C	C3C	−22.5(4)	C1C	N1C	C2C	C8C	100.3(4)
C1C	N1C	C4C	C5C	−7.8(6)	C1C	N2C	S1C	C12C	−75.1(3)
C1C	N2C	C3C	C2C	−21.9(4)	C2A	N1A	C4A	C5A	−174.2(3)
C2B	N1B	C4B	C5B	−168.1(3)	C2C	N1C	C4C	C5C	−173.4(4)
C3A	N2A	S1A	C12A	129.3(3)	C3A	C2A	N1A	C4A	144.2(3)
C3A	C2A	C8A	C9A	168.9(4)	C3A	C2A	C8A	C10A	−74.0(4)
C3A	C2A	C8A	C11A	47.3(5)	C3B	N2B	S1B	C12B	129.6(6)
C3B	C2B	N1B	C4B	141.7(3)	C3B	C2B	C8B	C19B	173.2(4)
C3B	C2B	C8B	C10B	−67.5(5)	C3B	C2B	C8B	C11B	52.5(5)
C3C	N2C	S1C	C12C	122.1(3)	C3C	C2C	N1C	C4C	145.0(3)
C3C	C2C	C8C	C9C	168.1(4)	C3C	C2C	C8C	C10C	−73.5(4)
C3C	C2C	C8C	C11C	46.9(5)	C4A	N1A	C2A	C8A	−94.3(4)
C4A	C5A	C6A	C7A	−173.9(4)	C4B	N1B	C2B	C8B	−94.7(4)
C4B	C5B	C6B	C7B	−173.8(5)	C4C	N1C	C2C	C8C	−92.3(4)
C4C	C5C	C6C	C7C	−173.4(5)	C12A	C13A	C14A	C15A	0.6(6)
C12A	C17A	C16A	C15A	−0.2(6)	C12B	C13B	C14B	C15B	1.3(6)
C12B	C17B	C16B	C15B	1.2(6)	C12C	C13C	C14C	C15C	−1.5(6)
C12C	C17C	C16C	C15C	−0.9(6)	C13A	C12A	C17A	C16A	2.7(5)
C13A	C12A	C17A	C20A	−176.8(4)	C13A	C14A	C15A	C16A	1.8(6)
C13A	C14A	C15A	C19A	−175.9(4)	C13B	C12B	C17B	C16B	−2.2(5)
C13B	C12B	C17B	C20B	177.4(4)	C13B	C14B	C15B	C16B	−2.3(6)
C13B	C14B	C15B	C19B	177.4(5)	C13C	C12C	C17C	C16C	3.0(6)
C13C	C12C	C17C	C20C	−177.4(4)	C13C	C14C	C15C	C16C	3.7(7)
C13C	C14C	C15C	C19C	−175.2(4)	C14A	C13A	C12A	C17A	−3.0(5)
C14A	C15A	C16A	C17A	−2.0(6)	C14B	C13B	C12B	C17B	1.0(5)
C14B	C15B	C16B	C17B	1.0(7)	C14C	C13C	C12C	C17C	1.9(6)
C14C	C15C	C16C	C17C	−2.4(7)	C15A	C14A	C13A	C18A	179.8(4)
C15A	C16A	C17A	C20A	179.4(4)	C15B	C14B	C13B	C18B	−179.4(4)
C15B	C16B	C17B	C20B	−178.5(4)	C15C	C14C	C13C	C18C	178.8(4)
C15C	C16C	C17C	C20C	179.5(4)	C17A	C12A	C13A	C18A	178.0(4)
C17A	C16A	C15A	C19A	175.6(4)	C17B	C12B	C13B	C18B	−178.2(4)
C17B	C16B	C15B	C19B	−178.7(4)	C17C	C12C	C13C	C18C	177.7(4)
C17C	C16C	C15C	C19C	176.5(4)					

steric congestion of the system, the 2-imidazolidinone rings in **3A**, **3B**, and **3C** were nonplanar and adopted distorted envelope conformation (half-chair; LISLOO). A common characteristic molecules **3A**, **3B**, and **3C** is the dihedral angle between *tert*-butyl and the 2-imidazolidinone rings, with values of −74.0° (**3A**), −67.5° (**3B**), and −73.5° (**3C**) [20, 43–46]. Similarly the dihedral angle between *n*-butyryl group and the 2-imidazolidinone rings is −9.6.0° (**3A**), −6.1° (**3B**), and −7.8° (**3C**) as expected in order to minimize unfavourable steric interactions between *tert*-butyl and *n*-butyryl moiety. Another common feature of the three molecules is the relative orientation of the *n*-butyryl. They adopt a *transoid* conformation and each *n*-butyryl group is nearly out of the plane of the corresponding 2-imidazolidinone (dihedral angles 6°~9°). A remarkable structural feature of the solid-state structures of molecules **3A**, **3B**, and **3C** is the bond angles, whereas the geometrical distortion is manifested in the smaller ∠C2–C3–N2 (102.2°) and ∠N1–C2–C3 (101.0°) bond angles (Figure 1, Table 3) [20, 38–41]. In addition, the structures of molecules **3A**, **3B**, and **3C** were superimposed in order to reveal the conformational differences of the three molecules (Figure 2). The strategy of overlay fit to match 2-imidazolidinone rings and examines any spatial differences between the atoms of the peripheral fragments. The results show that atoms of the *n*-butyryl, and 2,4,6-trimethylphenylsulfonyl groups occupy different spatial positions relative to the plane of 2-imidazolidinone ring which may explain the existence of such three molecules in one unit cell.

Table 5: Heat of formations, relative energies, dipole moments, and selected geometric parameters for the significant conformations of **3** computed using semiempirical AM1 MO level of theory. Comparative analysis with crystal structure **3**[a].

Property[a]	*Conformer* **A**[b,c]	*Conformer* **B**	*Conformer* **C**	*Conformer* **D**	*Conformer* **E**	*Conformer* **F**	X-ray **3A**	X-ray **3B**	X-ray **3C**
∠C1–N1–C4–C5	−23.8 (−**9.9**, −*40.8*)	−24.6	−28.0	−24.7	156.4	137.9	−9.6	−6.1	−7.8
∠C1–N2–S1–C12	−61.7 (−**46.2**, −*68.1*)	61.7	−109.1	136.3	−45.7	−107.7	−69.5	−65.9	−75.1
∠N2–S1–C12–C13	−81.5 (−**71.8**, −*75.2*)	−98.3	−97.7	−81.2	−80.3	83.7	−72.1	−72.7	−73.5
∠C3–C2–C8–C10	−65.9 (−**64.9**, −*55.1*)	−62.7	−63.9	−62.5	−66.8	−59.9	−74.0	−67.5	−73.5
∠C1–N1–C2	110.0 (**110.3**, *109.5*)	109.9	110.1	109.9	109.0	110.7	111.9	111.0	111.0
∠C1–N2–C3	108.8 (**112.4**, *108.6*)	108.7	108.8	108.8	108.7	108.8	111.1	111.3	111.0
N1–C4	1.410 (**1.39**, *1.45*)	1.410	1.41	1.41	1.41	1.41	1.408	1.401	1.413
N2–S1	1.67 (**1.68**, *1.79*)	1.67	1.67	1.67	1.67	1.66	1.777	1.664	1.669
S1–C12	1.68 (**1.80**, *1.79*)	1.68	1.69	1.69	1.67	1.69	1.671	1.773	1.768
Hf (kcal/mol)	−135.596	−135.069	−134.115	−132.739	128.334	127.122	—	—	—
Er (kcal/mol)	0.000	0.527	1.481	2.857	7.262	8.474	—	—	—
Dipole (Debye)	3.57	4.45	4.90	6.35	5.06	9.01	—	—	—

[a]All values correspond to fully optimized geometries.
[b]Relative energies for the three similar conformations resulted from the separate conformational analysis of **3A**, **3B,** and **3C** around the N1–C4 and N2–S1 bonds: 0.000, 0.110, and 0.05 kcal/mol, respectively.
[c]Values in bold, plain, and italic text corresponding to MM+, AM1, and PM3 geometry optimization, respectively.

To conclude, it is found that the solid state conformations of the three molecules of **3** (**3A**, **3B**, and **3C**) in the unit cell are quite similar, showing minor differences in some bond length and bond angle and major differences in some torsion angles at the peripheral substitution. However, and despite the high congestion in the molecular structures of these compounds, they form quiet molecular packing that likely reflects the subtle influence of the diverse intermolecular interactions.

The crystal packing of **3** is indicated in Figure 3. The molecules are arranged in a layer constituted by three molecules of **3A**, **3B**, and **3C** and that are maintained by numbers of CH-O, CH-π, and π-π interactions [45–47]. The main structural feature of the packing of **3** is that two molecules are quite parallel to each other and connected by π-π interactions of the two aryl fragments (5.03 Å) with coordinates −4.250, −2.462, and −0.875, while the third molecule was arranged in a lateral arrangement and approximately in opposite direction to the other two molecules. Additionally, the intramolecular interactions within each molecules of **3** involve O atom of sulfonyl fragment and hydrogen atoms from the CH_3 of 2,4,6-trimethylphenyl group (1.902–2.081 Å). The main putative interactions CH-O, as inferred by relatively short distances and suitable orientations, are indicated in Figure 3. On the basis of the short distances and the wide angle, the CH-O intermolecular interactions are likely to be quite strong and an important factor to determine the crystal packing; these bonds can be considered as nonclassical hydrogen bonds [45–47] involving CH as H-bond donors. Moreover, the third opposite molecule was showing CH-π interaction of the alkyl part of the butyryl moiety of this molecule and the aromatic fragment of the middle molecule (3.86 Å). Similarly the CH_3 group of the 2,4,6-trimethylbenzenesulfonyl group of the middle molecule interacted with aromatic moiety of the third opposite lateral molecule through CH-π interaction (3.60 Å). Finally, it must be indicated that the relative orientation between two parallel molecules of **3** in the crystal packing and the third opposite lateral molecule might indicate, besides steric suitability, a tendency to minimize the polarity of the crystal (compensating the dipole moments of the molecules) [48].

3.2. Computational Studies. Despite the interesting properties of the 1-arenesulfonyl-2-imidazolidinones, these compounds have been scarcely studied from a computational point of view [20, 49, 50]. Our goal was to compute quantum-chemical derived properties that would be useful as starting points for understanding the properties of this type of ring system. Moreover, the other main task of conformational

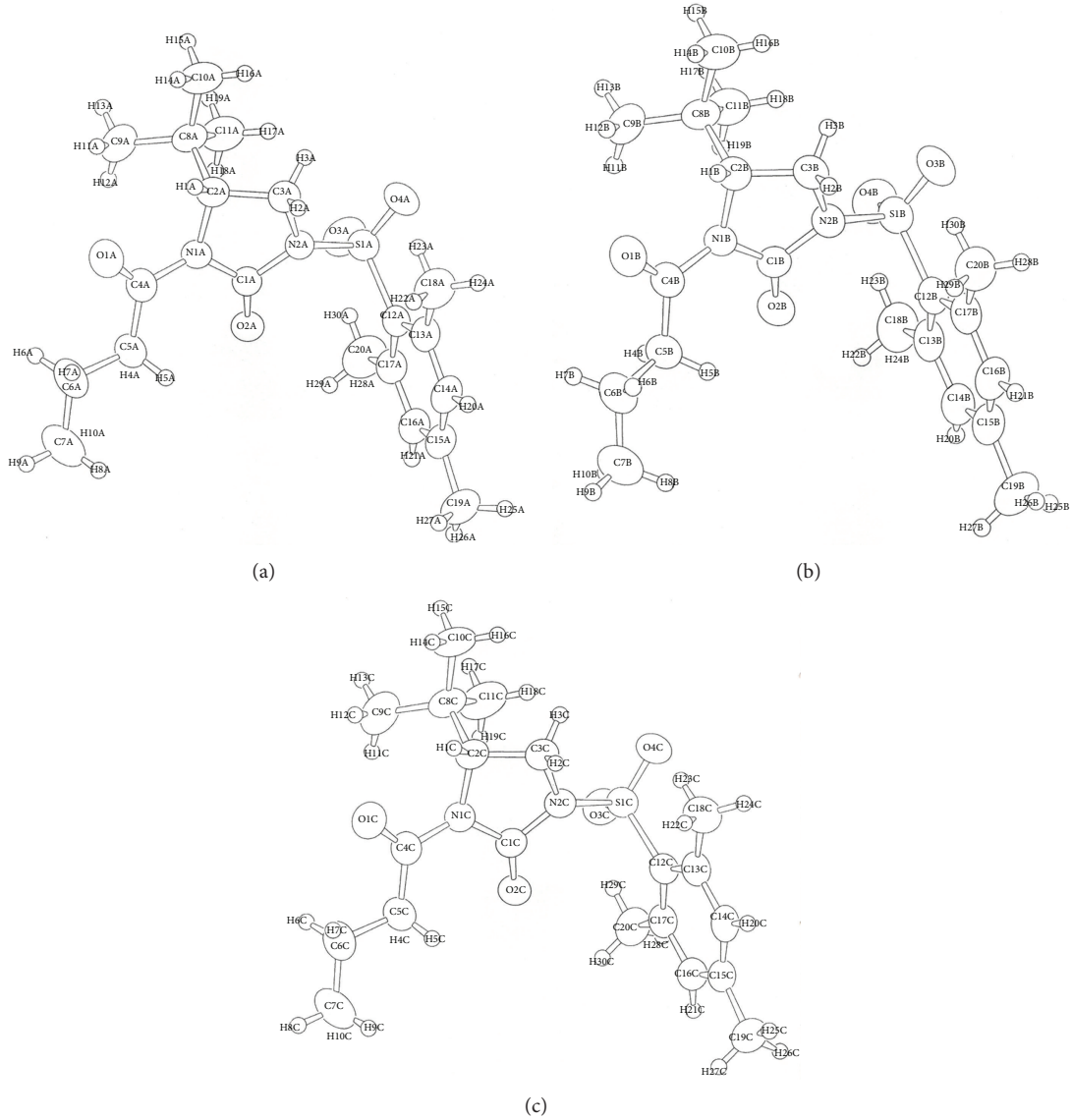

Figure 1: Numbering system of the three molecules (**3A**; (a), **3B**; (b), and **3C**; (c)) of the X-ray structure of compound **3**.

analyses of isolated molecules **3A**, **3B**, and **3C** was to examine the stable conformations and a global energy minimum for each molecule. If there was considerable energy difference between the lowest energy of **3A**, **3B**, and **3C** type of conformer, then we concluded that theoretical calculations predicted one type of geometric molecule. Since, the size and the variety of heteroatoms in the 2-imidazolidinones are considerable, a full semiempirical geometrical optimization is computationally very demanding. This work is simplified, if we use a realistic structure as starting geometry for the MM conformational search and quantum-chemical calculation. Therefore, the structures obtained by X-ray diffraction analysis are suitable to this end. Since compound **3** appears as three independent molecules in the asymmetric unit, the three structures (molecules **3A**, **3B**, and **3C**) were separately submitted to the conformational search using molecular mechanic MM+ and the energy minima conformer together with the highest energy conformer were subjected to full semiempirical AM1 and PM3 geometry optimization (Figures 4 and 5). Each conformer was confirmed as minimum or transition state on the basis of frequency calculation using AM1 results.

3.2.1. Theoretical Calculations. Taking into account our interest in the structural study of 2-imidazolidinone, the choice of computational methods which could reproduce the experimental data with reasonable agreement was relevant. Thus, we analyzed the conformational behaviour of compound **3** using semiempirical AM1 and PM3 quantum-chemical calculations. Conformational performance of the 2-imidazolidinone **3** was examined by the rotation and orientation in the space of the flexible *tert*-butyl, *n*-butyryl and 2,4,6-trimethylbenzenesulfonyl groups. Heat of formation,

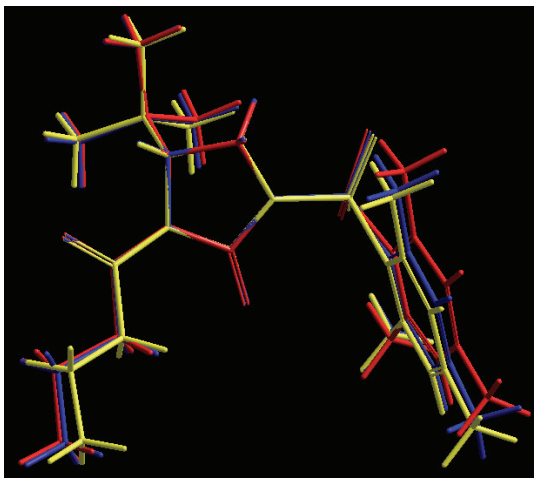

Figure 2: The superposition of the three molecules (molecule **3A**: colors blue, molecule **3B**: colors yellow, and molecule **3C**: colors red) of X-ray structure of compound **3**.

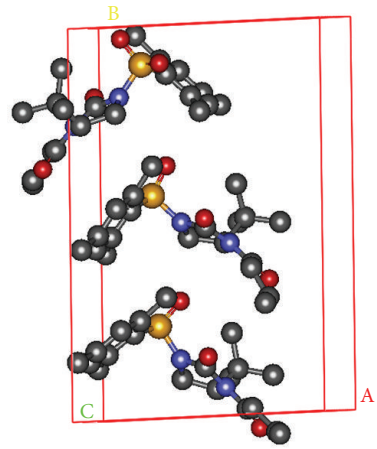

(a)

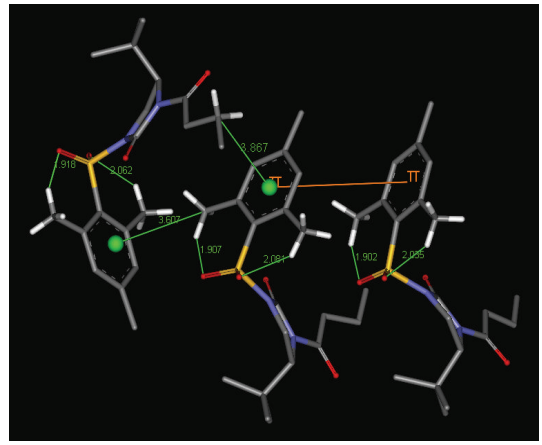

(b)

Figure 3: Crystal packing of compound **3** (a). (b) Shows intermolecular CH-O, CH-π (green lines), and π-π interactions (orange line). Hydrogen atoms are omitted for clarity except hydrogen included in CH-O interaction.

relative energies and dipole moment are collected in Table 5 and characteristic torsional angles, bond angles, and bond distance are also tabulated to illustrate the final geometries obtained. For such compound **3** the MM and semiempirical calculations led to six minimum energy conformations (Figures 4 and 5) within energy differences less than 8 kcal/mol (Table 5). Additionally, the molecular structure of compound **3** was determined by MM+ and semiempirical AM1 and PM3 calculations to assess the accuracy of the theoretical methods used for compound **3**. Conformations of the single molecules predicted by AM1, more than MM+ and PM3 methods, were approximately similar to that in the crystal (Figure 4).

The arrangement around the N2–S1 and N1–C4 bonds mainly determines the geometry of the *N*-substituent groups. Based on the geometrical comparison, these forms can be classified into two groups characterised by the torsion angle ∠C1–N1–C4–C5 denoted as *conformer*-**A**, -**B**, -**C** and -**D** for *transoid* butyryl fragment and *conformer*-**E** and -**F** for *cisoid* butyryl fragment (around −23.8° and 137.9°, resp.). For each group there are two or more possible orientations of the 2,4,6-trimethylbenzenesulfonyl moiety (torsion angle ∠C1–N2–S1–C12) with a similar energy content. However, the relative energy content of these conformers indicates a strong preference for conformations **A**-**B**, while the **C**-**F** forms are strongly destabilised. Therefore, it seems that the spatial orientations of the O=S=O of 2,4,6-trimethylbenzenesulfonyl and C=O of *n*-butyryl group relative to C=O of 2-imidazolidinone ring should be affecting the dipole moment as *trans*-orientation leads to a decrease of this force and vice versa. The high dipole moment represented by *cis* orientation probably due to the destabilising through-space interactions of the lone pairs of oxygen atoms yields much greater energy differences such as **C**-**F** conformations. In light of these findings, **A**-**B** conformations were more preferred compared with **C**-**F** conformations which are unfavourable and their participation may be negligible. Therefore, it seems that the orientation of *n*-butyryl group with 2,4,6-trimethylbenzenesulfonyl moiety exerts a significant effect on the conformational preferences of the compound **3** and this behaviour may be attributed to a combination of steric and electronic factors.

The AM1 method shows that the relative orientation of the aryl group of the most stable *conformer*-**A** is practically fixed in an anticonformation relative to position of *tert*-butyl fragment. These features are in concordance with the behaviour of reported molecules [17, 18]. Moreover, the aryl group can adopt two symmetric and isoenergetic conformations in which the *tert*-butyl and the aryl groups are *syn* and *anti*-positions (torsion angle ∠C1–N2–S1–C12 about −61.7, 61.7°). Moreover, the energy content of the three similar conformation of the *conformer*-**A** is very close with a slight predominance of the orientation of the 2,4,6-trimethylbenzenesulfonyl group as their interconversion requires a low cost (0.05 kcal/mol).

3.2.2. Comparison of the X-Ray and Calculated Structures. The crystal structure of **3** confirms the approximate behaviour of such compound in the gas phase (theoretical

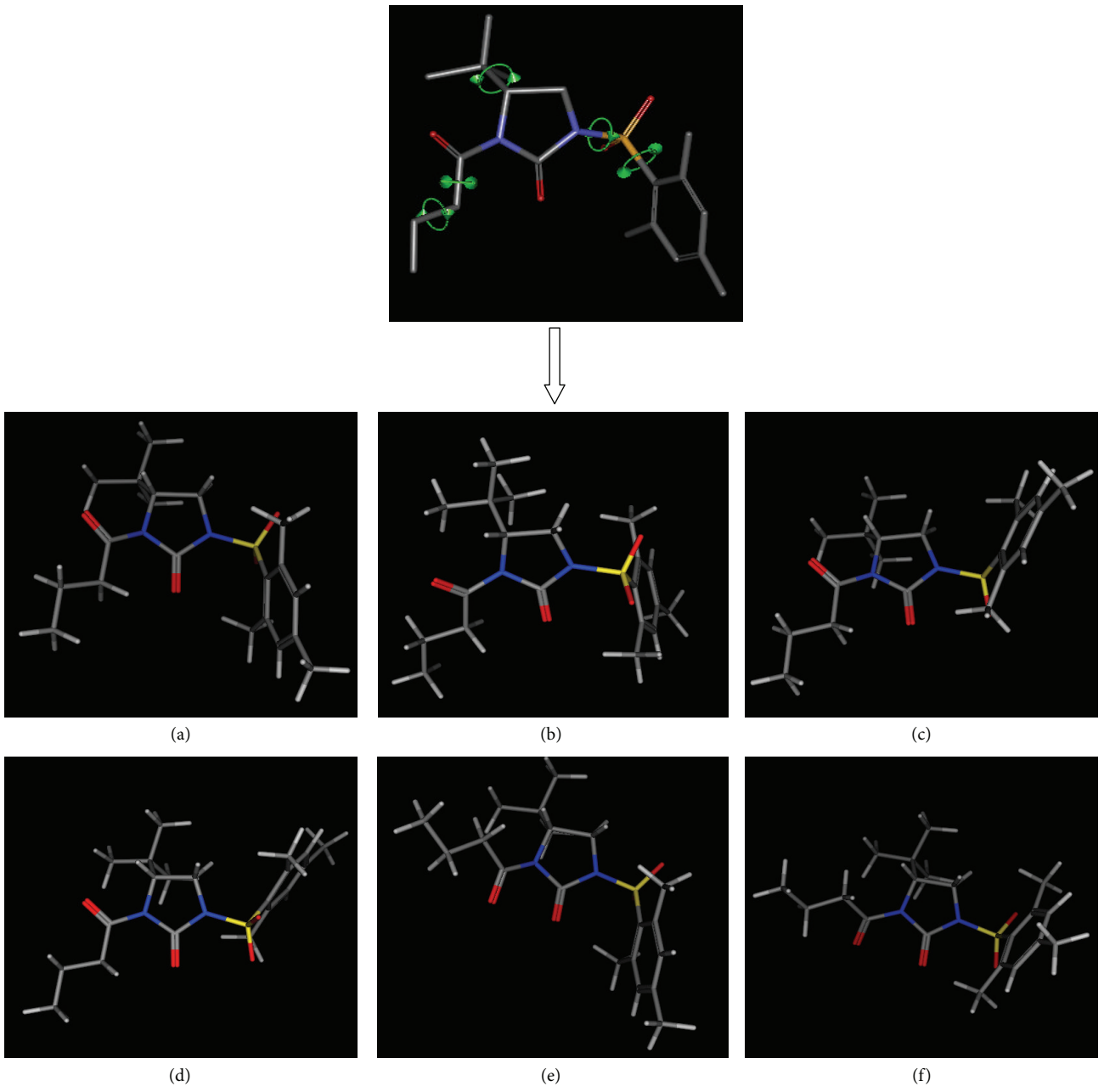

Figure 4: Results of conformational search showing most stable energy minimum: *conformer*-**A** (a), *conformer*-**B** (b), and the least stable conformers, including *conformer*-**C** (c), *conformer*-**D** (d), *conformer*-**E** (e), and *conformer*-**F** (f).

calculations). The good agreement between experimental torsion angles determined for **3** and those calculated for the *conformer*-**A** (Table 5) supports the correctness of the calculations. Because the barrier of energy of rotation of the three forms of *conformer*-**A** is very low so *conformer*-**A** was predicted representing all the three molecules of X-ray data. The low Gibbs energies of rotation between all possible *transoid* rotamers indicate the easy conversion between the three molecules in solution, and the solid state crystal structure was obtained in which it showed the important role of intermolecular interaction in stabilizing the molecules in solid states. The different disposition of the *n*-butyryl group (torsion angle ∠C1–N1–C4–C5 = −6.1~−9.6° in the solid state and −23.8° for the more favourable orientation computed using AM1 method) may be ascribed to the packing in the crystal structure. Similarily the different orientation of 2,4,6-trimethylbenzenesulfonyl (torsion angle ∠C1–N2–S1–C12 = −65.9° ~−75.1° in the solid state and −61.7° for the most stable *conformer*-**A** may be attributed to CH-O, CH-π, and π-π interactions in the crystal packing. Owing to theoretical calculations account for very low energy differences between the three dispositions around the N2–S1

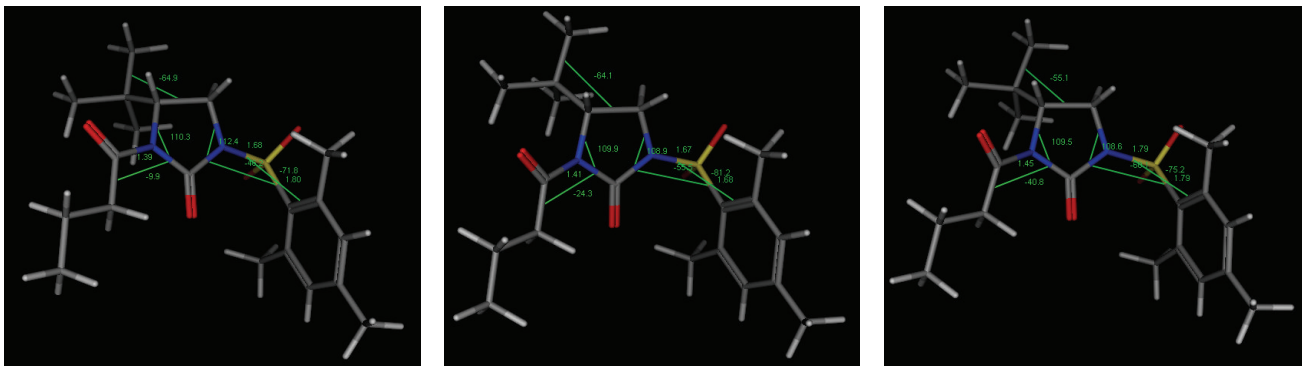

(a) (b) (c)

Figure 5: Most stable energy minimum (*conformer*-**A**) as energy optimized with MM+ force field (a) and both AM1 (b) and PM3 (c) semiempirical molecular orbital methods showing some geometrical parameters such as bond length, bond angle, and dihedral angle.

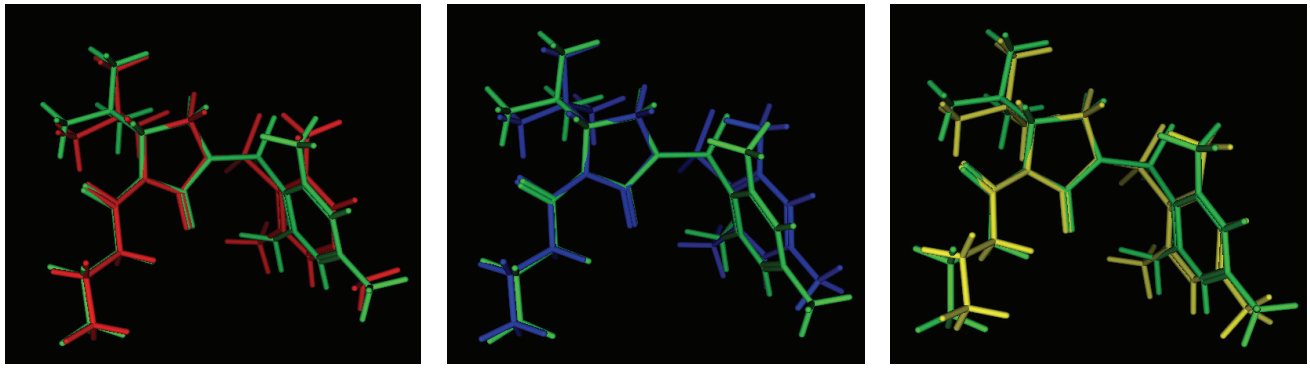

Figure 6: The superposition of the theoretical model (*conformer*-**A** (colors green))and the three molecules (molecule **3A**, colors blue, molecule **3B**: colors yellow, and molecule **3C**: colors red) of X-ray structure of compound **3**.

bond, their interconversion can take place easily. It was suggested that the change in the spatial orientation of the 2,4,6-trimethylbenzenesulfonyl group could be facilitated by the intermolecular interaction in the crystal structure. The *anti*-conformation of 2,4,6-trimethylbenzenesulfonyl adopted in the solid state relative to *tert*-butyl group would be more favourable for their formation due to the CH-O being sterically more accessible with lower dipole moment. These results confirm the flexibility of the 2,4,6-trimethylbenzenesulfonyl group in these 2-imidazolidinone derivatives and the strong dependence on intermolecular interactions as was previously suggested. Moreover, the great similarity between these conformers is the bond length with only 0.05 Å deviation among them. Hence, calculations at the semiempirical levels of the conformational energies of compound **3** indicate that the ideal gas-phase global energy minimum conformation is partially observed in the solid state. Rather, the effects of intermolecular interactions in the crystal structure cause the molecules to adopt higher-energy conformations, which correspond to local minima in the molecular potential energy surface. Finally to probe similarity and differences between the three-dimensional structures of the *conformer*-**A** and molecules **3A**, **3B**, and **3C**, molecular superposition has been performed (Figure 6). The strategy of overlay fit to match 2-imidazolidinone rings and examines any spatial differences between the atoms of the 4-*tert*-butyl, *n*-butyryl, and 2,4,6-trimethylbenzenesulfonyl. The results show that atoms of the 4-*tert*-butyl, butyryl, and arenesulfonyl groups occupy different spatial positions relative to each other as described above.

4. Conclusion

The crystal structures of (4*R*)-(−)-1-(2,4,6-trimethylbenzenesulfonyl)-3-*n*-butyryl-4-*tert*-butyl-2-imidazolidinone (**3**) were reported. This compound **3** crystallized in layers formed by crystallographic independent molecules. These crystallographic motifs are the consequence of the interplay of the diverse intermolecular interactions in the crystal packing. The crystal packing showed three molecules of compound **3** were stacked as a result of intermolecular interaction. A computational analysis of compound **3** was performed using the MM+ force field and fully optimized with semiempirical AM1 and PM3 MO methods. The comparison of experimental versus calculated values for the

selected bond lengths and angles of **3** is presented and the relative errors in calculated values are less than 3%. Both the experimental and calculated values agree that compound **3** is a sterically congested molecule. Theoretical conformational analyses have pointed out two factors that determine the conformation of the system under investigation. The first one is intermolecular interaction of the crystal packing, such as CH-O, CH-π, and π-π interactions, which stabilises and favours the occurrence of three independent molecules and the second factor is steric hindrance between substituents. The generally reasonable agreement between theoretical and experimental results have confirmed that the method which was applied for the theoretical conformational analysis of 2-imidazolidinone is good and useful for related organic molecules. Therefore, these results must be regarded as approximated and only with qualitative and comparative purposes. Moreover, the small differences between X-ray and calculated structures are consequence of different states of matter. During the theoretical calculation single isolated molecule is considered in vacuum, while many molecules are treated in solid state during X-ray diffraction. However, all the calculated geometric parameters, obtained by three used models (MM+, AM1, and PM3), represent good approximations and they can be applied as groundwork for prediction and exploring the other properties of the conformers.

5. Supporting Information Available

Crystallographic data for the structure in this paper have been deposited with the Cambridge Crystallographic Data Centre as the Supplementary Publication (no. CCDC 734938). Copies of the data can be obtained, free of charge, through application to CCDC, 12 Union Road, Cambridge CB2 1EZ, UK (fax: +44 1223 336033 or e-mail: deposit@ccdc.cam.ac.uk.

Conflict of Interests

The author(s) declare(s) that there is no conflict of interests regarding the publication of this paper.

Acknowledgment

The authors extend their appreciation to the Deanship of Scientific Research at King Saud University for funding work through the research group Project no. RGP-VPP-163.

References

[1] W. J. Hehre, *Dealing with Conformationally Flexible Molecules, Practical Strategies for Electronic Structure Calculations, Wavefunction*, chapter 6, 1995.

[2] H. Matsunaga, T. Ishizuka, and T. Kunieda, "Synthetic utility of five-membered heterocycles—chiral functionalization and applications," *Tetrahedron*, vol. 61, no. 34, pp. 8073–8094, 2005.

[3] N. Hashimoto, T. Ishizuka, and T. Kunieda, "Highly efficient chiral 2-oxazolidinone auxiliaries derived from methylcyclopentadienes and 2-oxazolone," *Tetrahedron Letters*, vol. 35, no. 5, pp. 721–724, 1994.

[4] A. A.-M. Abdel-Aziz, J. Okuno, S. Tanaka, T. Ishizuka, H. Matsunaga, and T. Kunieda, "An unusual enhancement of chiral induction by chiral 2-imidazolidinone auxiliaries," *Tetrahedron Letters*, vol. 41, no. 44, pp. 8533–8537, 2000.

[5] A. A.-M. Abdel-Aziz, H. Matsunaga, and T. Kunieda, "Unusual N-acylation of sterically congested trans-4,5-disubstituted 2-imidazolidinones: remarkably facile C–C bond formation," *Tetrahedron Letters*, vol. 42, no. 37, pp. 6565–6567, 2001.

[6] H.-Y. P. Choo, S. Choi, S. H. Jung, H. Y. Koh, and A. N. Pae, "The 3D-QSAR study of antitumor arylsulfonylimidazolidinone derivatives by CoMFA and CoMSIA," *Bioorganic & Medicinal Chemistry*, vol. 11, no. 21, pp. 4585–4589, 2003.

[7] S. H. Jung, J. S. Song, H. S. Lee, S. U. Choi, and C. O. Lee, "Synthesis and evaluation of cytotoxic activity of novel arylsulfonylimidazolidinones ," *Bioorganic & Medicinal Chemistry Letters*, vol. 6, no. 21, pp. 2553–2558, 1996.

[8] S. H. Jung, J. S. Song, H. S. Lee, S. U. Choi, and C. O. Lee, "Synthesis and evaluation of cytotoxicity of novel arylsulfonylimidazolidinones containing sulfonylurea pharmacophore," *Archives of Pharmacal Research*, vol. 19, no. 6, pp. 570–580, 1996.

[9] S. H. Jung and S. J. Kwak, "Planar structural requirement at 4-position of 1-arylsulfonyl-4-phenyl-4,5-dihydro-2-imidazolones for their cytotoxicity," *Archives of Pharmacal Research*, vol. 20, no. 3, pp. 283–287, 1997.

[10] S. Jung, H. Lee, J. Song et al., "Synthesis and antitumor activity of 4-phenyl-1-arylsulfonyl imidazolidinones," *Bioorganic and Medicinal Chemistry Letters*, vol. 8, no. 12, pp. 1547–1550, 1998.

[11] E. Y. Moon, S. K. Seong, S. H. Jung et al., "Antitumor activity of 4-phenyl-1-arylsulfonylimidazolidinone, DW2143," *Cancer Letters*, vol. 140, no. 1-2, pp. 177–187, 1999.

[12] E. Y. Moon, H. S. Hwang, C. H. Choi, S. H. Jung, and S. J. Yoon, "Effect of DW2282 on the induction of methemoglobinemia, hypoglycemia or WBC count and hematological changes," *Archives of Pharmacal Research*, vol. 22, no. 6, pp. 565–570, 1999.

[13] H. S. Hwang, E. Y. Moon, S. K. Seong et al., "Characterization of the anticancer activity of DW2282, a new anticancer agent," *Anticancer Research B*, vol. 19, no. 6, pp. 5087–5093, 1999.

[14] S. H. Jung, S. J. Kwak, N. D. Kim, S. U. Lee, and C. O. Lee, "Stereochemical requirement at 4-position of 4-phenyl-1-arylsulfonylimidazolidinones for their cytotoxicities," *Archives of Pharmacal Research*, vol. 23, no. 1, pp. 35–41, 2000.

[15] S. H. Lee, K. L. Park, S. U. Choi, C. O. Lee, and S. H. Jung, "Effect of substituents on benzenesulfonyl motif of 4-phenyl-1-arylsulfonylimidazolidinones for their cytotoxicity ," *Archives of Pharmacal Research*, vol. 23, no. 6, pp. 579–584, 2000.

[16] I. W. Kim and S. H. Jung, "Recognition of the importance of imidazolidinone motif for cytotoxicity of 4-phenyl-1-arylsulfonylimidazolidinones using thiadiazolidine-1,1 -dioxide analogs," *Archives of Pharmacal Research*, vol. 25, no. 4, pp. 421–427, 2002.

[17] I. Kim, C. Lee, H. Kim, and S. Jung, "Importance of sulfonylimidazolidinone motif of 4-phenyl-1-arylsulfonylimidazolidinones for their cytotoxicity: synthesis of 2-benzoyl-4-phenyl[1,2,5]thiazolidine-1,1-dioxides and their cytotoxcity," *Archives of Pharmacal Research*, vol. 26, no. 1, pp. 9–14, 2003.

[18] A. Guirado, R. Andreu, B. Martiz, D. Bautista, C. Ramírez de Arellano, and P. G. Jones, "The reaction of 4-amino-2-oxazolines with isocyanates and isothiocyanates. Synthesis and

X-ray structures of polysubstituted 2-imidazolidinones, 1,3-oxazolidines and 1,3-thiazolidines," *Tetrahedron*, vol. 62, no. 26, pp. 6172–6181, 2006.

[19] K.-L. Park, B.-G. Moon, S.-H. Jung, J.-G. Kim, and I.-H. Suh, "Multicentre hydrogen bonds in a 2:1 arylsulfonylimidazolone hydrochloride salt ," *Acta Crystallographica C*, vol. 56, pp. 1247–1250, 2000.

[20] A. A.-M. Abdel-Aziz, M. A. Al-Omar, A. S. El-Azab, and T. Kunieda, "Conformational preferences of sterically congested 2-imidazolidinone using X-ray analysis and computational studies. Part 1: *trans*-1-acetyl-4,5-di-*tert*-butyl-2-imidazolidinone," *Journal of Molecular Structure*, vol. 969, no. 1–3, pp. 145–154, 2010.

[21] I. A. Al-Swaidan, A. M. Alanazi, A. S. El-Azab, and A. A. -M. Abdel-Aziz, "An alternative route for synthesis of chiral 4-substituted 1-arenesulfonyl-2-imidazolidinones: unusual Utility of (4S,5S)- and (4R,5R)-4,5-dimethoxy-2-imidazolidinones and X-ray crystallography," *Journal of Chemistry*, vol. 2013, Article ID 349519, 5 pages, 2013.

[22] A. Altomare, M. C. Burla, M. Camalli et al., "SIR92-a program for automatic solution of crystal structures by direct methods," *Journal of Applied Crystallography*, vol. 27, p. 435, 1994.

[23] P. T. Beurskens, G. Admiraal, G. Beurskens et al., "DIRDIF 94: the DIRDIF-94 program system," Technical Report of the Crystallogtaphy Laboratory, University of Nijmegen, Nijmegen, The Netherlands, 1994.

[24] D. T. Cromer and J. T. Waber, *"International Tables for X-Ray Crystallography*, vol. 4, Table 2. 2 A, The Kynoch press, Birmingham, UK, 1974.

[25] J. A. Ibers and W. C. Hamilton, "Dispersion corrections and crystal structure refinements," *Acta Crystallographica*, vol. 17, pp. 781–782, 1964.

[26] D. C. Creagh and W. J. McAuley, *International Tables for Crystallography, Vol. C, (A.J.C.Wilson, Ed.)*, Table 4.2.6.8, Kluwer Academic, Boston, Mass, USA, 1992.

[27] "teXsan: Crystal Structure Analysis Package," Molecular Structure Corporation (1985 & 1992).

[28] Hypercube, *HyperChem: Molecular Modeling System*, Release 8.0.6, Hypercube, Gainesville, Fla, USA, 1995–2009.

[29] S. Profeta Jr. and N. L. Allinger, "Molecular mechanics calculations on aliphatic amines," *Journal of the American Chemical Society*, vol. 107, no. 7, pp. 1907–1918, 1985.

[30] M. Lipton and W. C. Still, "The multiple minimum problem in molecular modeling. Tree searching internal coordinate conformational space," *Journal of Computational Chemistry*, vol. 9, no. 4, pp. 345–355, 1988.

[31] A. A.-M. Abdel-Aziz, "Novel and versatile methodology for synthesis of cyclic imides and evaluation of their cytotoxic, DNA binding, apoptotic inducing activities and molecular modeling study," *European Journal of Medicinal Chemistry*, vol. 42, no. 5, pp. 614–626, 2007.

[32] M. J. S. Dewar, E. G. Zoebisch, E. F. Healey, and J. J. P. Stewart, "Development and use of quantum mechanical molecular models. 76. AM1: a new general purpose quantum mechanical molecular model," *Journal of the American Chemical Society*, vol. 107, no. 13, pp. 3902–3909, 1985.

[33] J. J. P. Stewart, "Optimization of parameters for semiempirical methods I. Method," *Journal of Computational Chemistry*, vol. 10, no. 2, pp. 209–220, 1989.

[34] http://openmopac.net/home.html.

[35] J. W. Steed, "Should solid-state molecular packing have to obey the rules of crystallographic symmetry?" *Crystal Engineering Communications*, vol. 5, pp. 169–179, 2003.

[36] http://www.ccdc.cam.ac.uk/free_services/teaching/modules/ .

[37] J. L. Flippen, "The crystal and molecular structures of reaction products from -irradiation of thymine and cytosine: *cis*-thymine glycol, C5H8N2O4, and *trans*-1-carbamoylimidazolidone-4,5-diol, C4H7N3O4," *Acta Crystallographica B*, vol. 29, pp. 1756–1762, 1973.

[38] H. Ueda, H. Onishi, and T. Nagai, "Structure of *p*-aminobenzoic acidi-1,3-dimethyl-2-imidazolidinone (1/1)," *Acta Crystallographica C*, vol. 42, pp. 462–464, 1986.

[39] M. Kapon and G. M. Reisner, "Structure of 2-imidazolidinone hemihydrate," *Acta Crystallographica C*, vol. 45, pp. 780–782, 1989.

[40] O. M. Peeters, N. M. Blaton, and C. J. De Ranter, "Structure of 1-(5-nitro-1,3-thiazol-2-yl)-2-imidazolidinone (niridazole), C6H6N4O3S ," *Acta Crystallographica C*, vol. 40, pp. 1748–1750, 1984.

[41] F. H. Allen, O. Kennard, D. G. Watson, L. Brammer, A. G. Orpen, and R. Taylor, "Tables of bond lengths determined by x-ray and neutron diffraction. Part 1. Bond lengths in organic compounds," *Journal of the Chemical Society*, no. 12, pp. S1–S19, 1987.

[42] A. Caron, "Redetermination of thermal motion and interatomic distances in urea ," *Acta Crystallographica B*, vol. 25, p. 404, 1969.

[43] P. Vaughan and J. Donohue, "The structure of urea. Interatomic distances and resonance in urea and related compounds ," *Acta Crystallographica*, vol. 5, pp. 530–535, 1952.

[44] A. Caron and J. Donohue, "Three-dimensional refinement of urea," *Acta Crystallographica*, vol. 17, pp. 544–546, 1964.

[45] Y. Umezawa, S. Tsuboyama, H. Takahashi, J. Uzawa, and M. Nishio, "CH/π interaction in the conformation of organic compounds. A database study," *Tetrahedron*, vol. 55, no. 33, pp. 10047–10056, 1999.

[46] U. El-Ayaan, A. A.-M. Abdel-Aziz, and S. Al-Shihry, "Solvatochromism, DNA binding, antitumor activity and molecular modeling study of mixed-ligand copper(II) complexes containing the bulky ligand: bis[*N*-(*p*-tolyl)imino]acenaphthene," *European Journal of Medicinal Chemistry*, vol. 42, no. 11-12, pp. 1325–1333, 2007.

[47] U. El-Ayaan and A. A.-M. Abdel-Aziz, "Synthesis, antimicrobial activity and molecular modeling of cobalt and nickel complexes containing the bulky ligand: *bis*[*N*-(2,6-diisopropylphenyl)imino] acenaphthene," *European Journal of Medicinal Chemistry*, vol. 40, no. 12, pp. 1214–1221, 2005.

[48] G. R. Desiraju, J. A. R. P. Sarma, and T. S. R. Krishna, "Dipole-dipole interactions and the inversion motif in the crystal structures of planar chloro aromatics: the unusual packings of 1,2,3-trichlorobenzene and 1,2,3,7,8,9-hexachlorodibenzo-*p*-dioxin," *Chemical Physics Letters*, vol. 131, no. 1-2, pp. 124–128, 1986.

[49] J. C. Burley, R. Gilmour, T. J. Prior, and G. M. Day, "Structural diversity in imidazolidinone organocatalysts: a synchrotron and computational study ," *Acta Crystallographica C*, vol. 64, pp. o10–o14, 2008.

[50] A. G. Santos, S. X. Candeias, C. A. M. Afonso et al., "Rationalising diastereoselection in the dynamic kinetic resolution of α-haloacyl imidazolidinones: a theoretical approach," *Tetrahedron*, vol. 57, no. 30, pp. 6607–6614, 2001.